J Mater Sci (2011) 46:2541–2547
DOI 10.1007/s10853-010-5106-z

Interaction study of indigo carmine with albumin and dextran by NMR relaxation

Claudia Bonechi · Silvia Martini · Claudio Rossi

Received: 30 September 2010 / Accepted: 20 November 2010 / Published online: 4 December 2010

Abstract In this study, the interaction processes between a dye (indigo carmine) and two different macromolecular models were studied with the aim to obtain physical-chemistry information about the dyeing of textiles. Two macromolecules, albumin and dextran (DX), were chosen to simulate wool and cotton fibers during the coloration procedure in water. Proton NMR selective and non-selective spin–lattice relaxation rate measurements were used to monitor the strength of the overall complexation behavior of indigo carmine toward albumin or DX. The *affinity index*, a quantitative parameter related to the strength of the ligand–macromolecule interaction, was determined from selective spin–lattice relaxation rate enhancements due to the bound ligand molar fraction. Moreover, this approach allowed the calculation of the equilibrium constant of the complex formation (K) between the dye and macromolecular models. NMR data suggested a higher indigo carmine–albumin complex thermodynamic stability with respect to the indigo carmine–DX adduct. These results indicate a stronger persistence of the dyeing process in wool with respect to cotton fibers, in agreement with literature data.

Introduction

The textile dyeing industry has been in existence for more than 4,000 years [1]. For all but the last 150 years, the dyes were obtained from natural sources [2]. In particular, the natural textile was divided in two categories: animal and vegetable fibers. Wool is the fiber from the fleece of the domesticated sheep. It is a natural protein (85% keratin), staple fiber density of wool is 1.31 g/cm^3, which tends to make wool a medium weight fabric. Wool fiber may be varying from offwhite to light cream in color, which is due to the disulfide bond, acting as chromophores [3]. Cotton is a natural fiber (85% cellulose) that grows in a ball around the seeds of the cotton plant (*Gossypium)*. It is a shrub native to tropical and subtropical regions around the world. The fiber is used to make a soft, breathable textile, which is the most widely used natural-fiber cloth in clothing today.

The aim of this article was to investigate the dyeing textile process in water solution using macromolecular models able to simulate wool and cotton fibers. For this purpose, we chose albumin and dextran (DX) and a dye (indigo carmine), which show a good water solubility.

Serum albumin is the most abundant plasma protein, with a molecular weight of 66.2 kDa, that facilitates the disposition and transportation of various endogenous and exogenous ligands including fatty acids, steroids, metal ions, etc. [4–6]. Albumin is an acidic, very soluble, and extremely robust protein: it is stable in the pH range of 4–9, soluble in 40% ethanol, and can be heated at 60 °C for up to 10 h without deleterious effects. The absorption, distribution, metabolism, excretion properties as well as the stability and toxicity of fatty acids and dyes can be significantly affected as a result of their binding to serum albumins [7]. The three-dimensional structure of human serum albumin (HAS) has been elucidated by X-ray structure analysis [8], which consists of three structurally homologous, predominantly helical domains (domains I, II, and III). Moreover, there is evidence of conformational changes of serum albumin induced by its interaction with

C. Bonechi (✉) · S. Martini · C. Rossi
Department of Pharmaceutical and Applied Chemistry, University of Siena, Via Aldo Moro, 2 53100 Siena, Italy
e-mail: cbonechi@unisi.it

C. Bonechi · S. Martini · C. Rossi
Center for Colloid and Surface Science (CSGI), Via della Lastruccia 3, Sesto Fiorentino (FI), Italy

low molecular weight dyes and drugs, which appears to affect the secondary and tertiary structure of albumins [9]. Consequently, the investigation on the interaction of dyes and drugs with serum albumin is of great importance. Investigation on the interaction of bovine serum albumin (BSA) with a dye can help us to better understand the chemical absorption and distribution of dye, and hence become an important research field in chemistry.

Dextrans are hydrophilic and non-charged natural polysaccharides which are soluble in water in any proportion. The straight chain consists of α-1,6 glycosidic linkages between glucose molecules. DXs are also frequently used for biomedical and biophysical applications.

Natural dyes have been classified in relation to application mechanisms. The dye is generally applied in an aqueous solution, and may require a mordant to improve the fastness of the dye on the fiber. Vat dyes are essentially insoluble in water and incapable of dyeing fibers directly. However, reduction in alkaline liquor produces the water soluble alkali metal salt of the dye, which, in this leuco form, has an affinity for the textile fiber. Subsequent oxidation reforms the original insoluble dye.

Indigo is a vat dye which was probably one of the oldest-known coloring agent [10, 11]. Evidence of the use of indigoid dyes dates back to 2000 BC in Egypt. It has been used to dye cellulosic textiles, especially cotton. The major constituent of the indigo dye is indigotin. Indigo bearing plants can be found all over the world and the chemistry of this vat dyestuff renders it compatible with all natural fibers [12]. This blue dye is still employed extensively today for dyeing cotton yarn in the manufacture of denims and blue jeans. Since this dye is insoluble in water, it is necessary to reduce it to its leucosoluble form using a suitable reducing agent with an alkali, such as sodium hydroxide. When the preparation of leuco-indigo is achieved, the textile is dipped with the reduced dye. Then, the textile is exposed to air to oxidize the dye back to its insoluble form. These two steps (dipping/exposing) would be repeated many times to obtain the desired shade.

Indigo carmine (Fig. 1) is an anionic, synthetic dye of the indigoid group that is of great importance in food, drug, and cosmetic industries and [13, 14], photocatalytic processes[15]. It has been used as an indicator in analytical chemistry, as a food additive, as a microscopic stain in biological studies, and as a diagnostic drug [16].

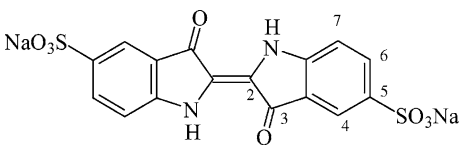

Fig. 1 Molecular structure and numbering of indigo carmine

In this article, the interaction of BSA and DX with indigo carmine was investigated via nuclear magnetic resonance (NMR) spectroscopy using proton selective and non-selective spin–lattice relaxation rate measurements. The analysis of the reciprocal of proton selective relaxation rate enhancements due to the occurring of interaction processes in relation to dye concentration, allowed the calculation of the complex thermodynamic equilibrium constant, K, and the relaxation rate of the dye bound to the macromolecule models. The results clearly demonstrated a stronger interaction between indigo and BSA with respect to dextran, i.e., a greater persistence of the dye on wool compared to cotton fibers. The approach we propose in this study, able to easily compare the ability of a dye to interact with different fiber constituents, may represent a contribution for understanding the efficiency of industrial processes of dyeing textile.

Experimental

Materials

Indigo carmine (3,3′-dioxo-2,2′-bis-indolyden-5,5′-disulfonic acid disodium salt), bovine serum albumin (BSA, molecular weight 66.2 kD) and dextran (DX, molecular weight 70.0 kDa) were purchased from Sigma Chemical Co., and used without any further purification. The dye indigo carmine is a purple colored, water soluble powder with molecular weight 466.36 kD. It was obtained from Merck and used as procured. Deuterium oxide, D_2O (99.98%) was purchased from Merck. In all the experiments the indigo concentration was 1.8×10^{-2} mol dm^{-3}.

NMR measurements

The solutions for the NMR experiments were obtained by dissolving the appropriate amounts of ligand indigo and protein macromolecules (BSA and dextran) in D_2O.

All the ^1H spectra were recorded on a Bruker 400 AMX spectrometer operating at 400 MHz. Spin–lattice relaxation rates were measured using the "inversion recovery" (180°-τ-90°-t)n sequence. The τ values used for the selective and non-selective experiments were: 0.01, 0.02, 0.04, 0.06, 0.08, 0.1, 0.2, 0.4, 0.8, 1, 1.5, 2, 3, 4, 5, 7, and 20 s respectively, and the delay time t in this case was 20 s. The 180° selective inversion of the proton spin population was obtained by a selective soft gaussian perturbation pulse (width: 60 ms, power: 120 dB) [17]. The FID was processed using an exponential window function with line broadening of 1 Hz. All the selective and non-selective spin–lattice relaxation rates refer to the aromatic proton (H6/7) of indigo carmine (Fig. 2). Since in general the

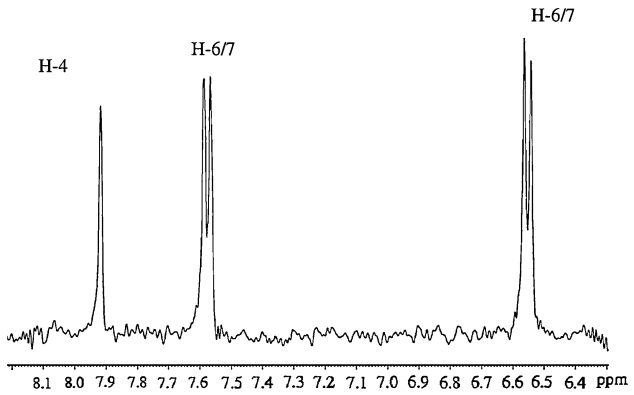

Fig. 2 400 MHz NMR proton spectrum of 1.8×10^{-2} mol dm^{-3} indigo carmine in D_2O solution at 298 K

recovery of proton longitudinal magnetization after a 180° pulse is not a single exponential, due to the sum of different relaxation terms, the selective spin–lattice relaxation rates were calculated using the initial slope approximation and subsequent three parameter exponential regression analysis of the longitudinal recovery curves. The maximum experimental error in the relaxation rate measurements was 5%. The affinity index was calculated by linear regression analysis of the experimental data.

All the spectra were processed using the Bruker Software XWINNMR, version 2.5 on Silicon Graphics O_2 equipped with RISC R5000 processor, working under the IRIX 6.3 operating system.

Theory

The explicit forms of non selective R_1^{NS} and selective R_1^{SE} proton spin–lattice relaxation rates are [18–23]:

$$R_1^{NS} = \frac{1}{10}\frac{\gamma_H^4\hbar^2}{r_{ij}^6}\left[\frac{3\tau_c}{1+\omega_H^2\tau_c^2}+\frac{12\tau_c}{1+4\omega_H^2\tau_c^2}\right] \quad (1)$$

$$R_1^{SE} = \frac{1}{10}\frac{\gamma_H^4\hbar^2}{r_{ij}^6}\left[\frac{3\tau_c}{1+\omega_H^2\tau_c^2}+\frac{6\tau_c}{1+4\omega_H^2\tau_c^2}+\tau_c\right] \quad (2)$$

R_1^{SE} and R_1^{NS} depend on ligand dynamics with different extent: $R_1^{NS} > R_1^{SE}$ in the fast molecular reorientation typical of the free ligand ($\omega_0\tau_c \ll 1$) and $R_1^{SE} > R_1^{NS}$ when the ligand is bound to a macromolecule ($\omega_0\tau_c \gg 1$).

Since the ligand NMR parameter most affected by drastic changes in the molecular dynamics is R_1^{SE}, it appears to be the best experimental parameter for obtaining information about ligand–macromolecule interactions. In conditions of fast chemical exchange between the free and bound environments, R_1^{SE} is expressed by the following equation:

$$R_{1obs}^{SE} = \chi_f R_{1f}^{SE} + \chi_b R_{1b}^{SE}, \quad (3)$$

where R_{1obs}^{SE} is the experimentally determined selective relaxation rate R_{1f}^{SE} and χ_f and R_{1b}^{SE} and χ_b are the selective spin–lattice relaxation rates and the ligand fractions of the free and bound environments, respectively.

If we consider the ligand–macromolecule equilibrium:

$$M + L \rightleftarrows ML \quad (4)$$

with an equilibrium constant $K = \frac{[ML]}{[M][L]}$ assuming $[L] \gg [M_0]$, it has been shown that:

$$\Delta R_1^{SE} = \frac{KR_{1b}}{1+K[L]}[M_0], \quad (5)$$

where $\Delta R_1^{SE} = R_{1obs}^{SE} - R_{1f}^{SE}$, K is the thermodynamic equilibrium constant, and $[M_0]$ is the initial macromolecule concentration. As suggested by Eq. 5, the plot ΔR_1 versus $[M_0]$ would have a straight line, with slope:

$$[A]_L^T = \left(\frac{KR_{1b}}{1+K[L]}\right), \quad (6)$$

which was defined as ≪*affinity index*≫ (dm^3 mol^{-1}s^{-1}). The affinity index is constant if temperature and ligand concentration are specified, as suggested by the T and L subscripts in the affinity index symbol.

Differences in the dynamics of portions of the molecule due to different correlation times modulating the dipolar interactions between protons at different positions, which may affect selective relaxation rates and as a consequence, the affinity index value, must be taken into account. The normalization of $\Delta R_1^{SE} = R_{1obs}^{SE} - R_{1f}^{SE}$ to R_{1f}^{SE} removes the effects of different correlation times and different proton densities and isolates the effects of restricted motions due to the interaction of the ligand with the macromolecule, leading to a normalized affinity index [24]:

$$\Delta R_{1N}^{SE} = \frac{KR_{1b}^{SE}[M_0]}{(1+K[L])R_{1f}^{SE}}. \quad (7)$$

The dependence of the normalized relaxation rate enhancements ΔR_{1N}^{SE} from the concentration of the macromolecule $[M_0]$ is represented by a straight line passing through the origin of the axes with slope:

$$\left[A_I^N\right]_L^T = \frac{KR_{1b}^{SE}}{(1+K[L])R_{1f}^{SE}}. \quad (8)$$

$\left[A_I^N\right]_L^T$ is still a constant at fixed temperature and ligand concentration and it is defined as "*normalized affinity index*" (dm^3 mol^{-1}).

Calculation of K and R_{1b}^{SE}

Eq. 7 may be rewritten as:

$$\frac{1}{\Delta R_{1N}^{SE}} = \frac{(1 + K[L])R_{1f}^{SE}}{KR_{1b}^{SE}[M_0]} \quad (9)$$

and:

$$\frac{1}{\Delta R_{1N}^{SE}} = \frac{R_{1f}^{SE}}{KR_{1b}^{SE}[M_0]} + \frac{[L]R_{1f}^{SE}}{R_{1b}^{SE}[M_0]}. \quad (10)$$

Plotting $1/\Delta R_{1N}^{SE}$ in relation to ligand concentration $[L]$ we should observe a linear behavior in which the slope and the intercept of the straight line are given by:

$$S = \frac{R_{1f}^{SE}}{R_{1b}^{SE}[M_0]} \quad (11)$$

and

$$I = \frac{R_{1f}^{SE}}{KR_{1b}^{SE}[M_0]}. \quad (12)$$

Since the concentration of the macromolecule is known and the relaxation rate of the free ligand can be directly measured, the relaxation rate of the bound ligand can be calculated using Eq. 11. R_{1b}^{SE} can be used to obtain the value of the equilibrium constant K from Eq. 12.

Results and discussion

The aromatic region of the proton NMR spectrum of indigo carmine in D_2O solution is displayed in Fig. 2.

Resonance assignments were checked by two-dimensional COSY and NOESY experiments (data not shown), nevertheless it was not possible to univocally assign the aromatic protons H6 and H7. The signal at 6.55 ppm was used for the selective and non-selective relaxation rate measurements.

Indigo–BSA interaction study

Table 1 reports the values of R_1^{SE} and R_1^{NS} of the H6/7 proton of indigo carmine in relation to albumin concentration.

Table 1 R_1^{SE} and R_1^{NS} values calculated for the H6/7 proton of indaco carmine (1.8×10^{-2} mol dm^{-3}) in the presence of variable albumin concentrations at 298 K

Albumin concentration (mg/mL)	Albumin concentration (mol dm^{-3})	R_1^{SE} (s^{-1})	R_1^{NS} (s^{-1})
0	0	0.43	0.51
1	1.51×10^{-5}	0.53	0.53
3	4.53×10^{-5}	0.75	0.54
5	7.55×10^{-5}	0.95	0.56
8	1.21×10^{-4}	1.28	0.73

The first evidence was that, in the absence of albumin, R_1^{NS} was bigger than R_1^{SE}. This result permits to confirm that indigo carmine (without protein) show fast reorientational motions in solution. These dynamical conditions allow the interaction processes to be investigated through the analysis of the selective and non-selective spin–lattice relaxation rates of the ligands.

The second evidence was that with the increase of albumin concentration R_1^{NS} values remained constant while R_1^{SE} increased. The selective relaxation rate enhancements reveal the existence of a large contribution from the bound ligand fraction to the observed relaxation rate, which suggests the presence of an interaction between the colorant and BSA.

However, solutions containing relatively high concentrations of protein may be subject to an increase in viscosity and this phenomenon may cause a slow down in the dynamics of the ligand even in the absence of an interaction with the protein. In order to investigate this phenomenon, the non-selective spin–lattice relation rate versus temperature was analysed and data was reported in numerous previous article [25, 26].

In order to evaluate the strength of the interaction between the ligand, indigo carmine, and BSA, the normalized affinity index $[A^N]_L^T$ was calculated from the slope of the straight line obtained by H6/7 normalized selective relaxation enhancements, ΔR_{N1}^{SE}, as a function of protein concentration. As reported in the theory section, the normalized affinity index allows to remove the effects of motional anisotropies along the ligand molecule and differences in the magnetic environment to the experimental spin–lattice relaxation rate values.

Figure 3 shows the linear regression analysis of normalized selective relaxation rate enhancements of indigo

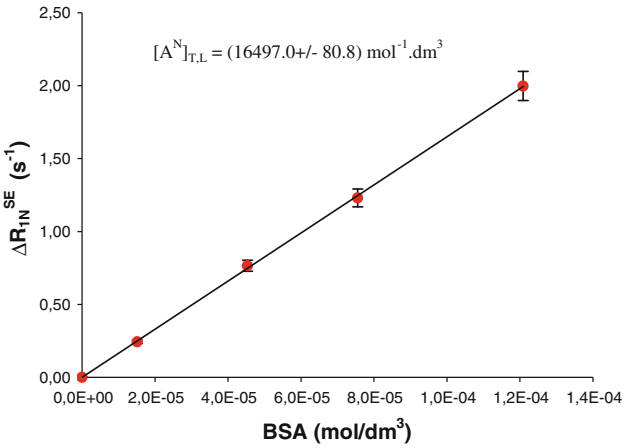

Fig. 3 Linear regression of the H6/7 normalized selective relaxation enhancement, ΔR_{N1}^{SE}, as a function of albumin concentration of a solution of indigo carmine. The values of the normalized affinity indexes $[A^N]_L^T$ (mol^{-1} dm^3) are also reported with the corresponding errors (5%)

carmine, ΔR_{N1}^{SE}, as a function of BSA concentration. The $[A^N]_L^T$ value was found to be (16497.0 ± 80.8) mol^{-1} dm^3.

Indigo–dextran interaction study

In order to study the interaction processes between the same dye, indigo carmine, and a different macromolecule, dextran, the experimental approach proposed above was used. Table 2 reports the values of R_1^{SE} and R_1^{NS} of the H6/7 proton of indigo carmine in relation to DX concentration.

These experimental data show that the condition $R_1^{NS} > R_1^{SE}$ was respected in the absence of dextran. From these data it is also evident that R_1^{NS} is practically unaffected by the presence of the macromolecule, whereas R_1^{SE} increases with increasing dextran concentration.

Figure 4 shows a plot of ΔR_{N1}^{SE} versus dextran concentration; the slope of the straight line obtained by linear regression analysis of the experimental points gave a normalized affinity index value of (1121.8 ± 85.7) mol^{-1} dm^3.

Table 2 Selective and non-selective spin–lattice relation rates for H6/7 of indigo carmine (1.8×10^{-2} mol dm^{-3}) versus dextran concentration at 298 K

Dextran concentration (mg/mL)	Dextran concentration (mol dm^{-3})	R_1^{SE} (s^{-1})	R_1^{NS} (s^{-1})
0	0	0.43	0.45
1	1.43×10^{-5}	0.44	0.43
3	4.29×10^{-5}	0.45	0.43
5	7.14×10^{-5}	0.46	0.44
8	1.14×10^{-4}	0.48	0.45

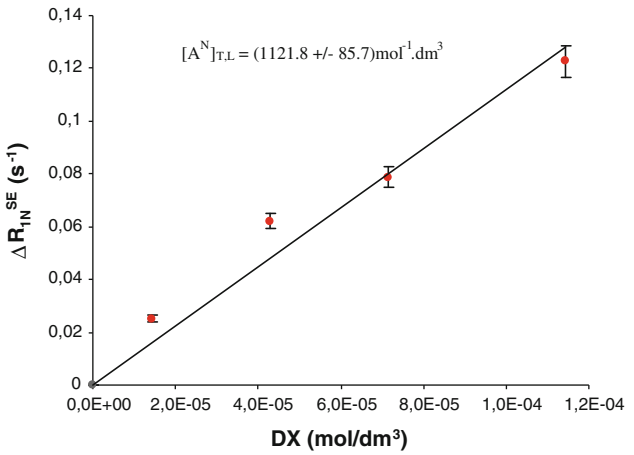

Fig. 4 Linear regression of the H6/7 normalized selective relaxation enhancement, ΔR_{N1}^{SE}, of a 1.8×10^{-2} mol dm^{-3} solution of indigo carmine as a function of dextran concentration. The values of the normalized affinity indexes $[A^N]_L^T$ (mol^{-1} dm^3) are also reported with the corresponding errors (5%)

The comparison between the affinity indexes calculated for the two dye-macromolecule systems (Fig. 5), indicate that indigo carmine has a stronger affinity for BSA with respect to DX. $[A^N]_L^T$ of indigo–BSA system was 15 times the indigo–DX affinity index. This behavior is in agreement with other studies concerning the investigation of the interaction of cotton and wool with dye [27, 28] It is clear, in fact, that the structure of the dye plays a key role in affecting their recognition processes with proteins and polysaccharides [29, 30] In particular, indigo carmine interacts mainly via hydrophobic interactions, which are stronger for albumin, with respect to dextran.

Equilibrium constant determination (K)

The analysis of the thermodynamics of complex formation constitutes an important step to deeply understand the properties of dye-macromolecule adducts, in terms of complex stability. In order to calculate the values of the complexation equilibrium constant (K), selective relaxation rates of indigo carmine were measured at different concentrations in the presence of a constant amount of BSA and DX. Figure 6 shows the calculated values of $1/\Delta R_1^{SE}$ of the indigo carmine measured at different concentrations in the presence of (a) BSA and (b) DX.

Using the values of the calculated slopes and applying Eq. 11, R_{1b}^{SE} was calculated as (141.7 ± 1.1) s^{-1} for indigo carmine–BSA complex, and (16.0 ± 1.3) $s^{-1}$for indigo carmine–DX complex. These data allowed the calculation of the equilibrium constants associated to the complex formation, which were found to be: (1500.6 ± 156.0) mol^{-1} dm^3 and (121.0 ± 15.0) mol^{-1} dm^3 for indigo carmine–BSA and for indigo carmine–DX, respectively. These results show that indigo was able to form more stable complexes

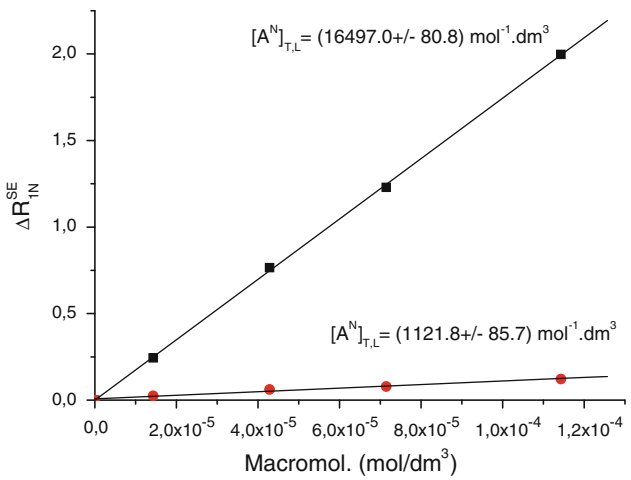

Fig. 5 Comparison between ΔR_{N1}^{SE} versus macromolecular concentration in presence of indigo carmine (1.8×10^{-2} mol dm^{-3})

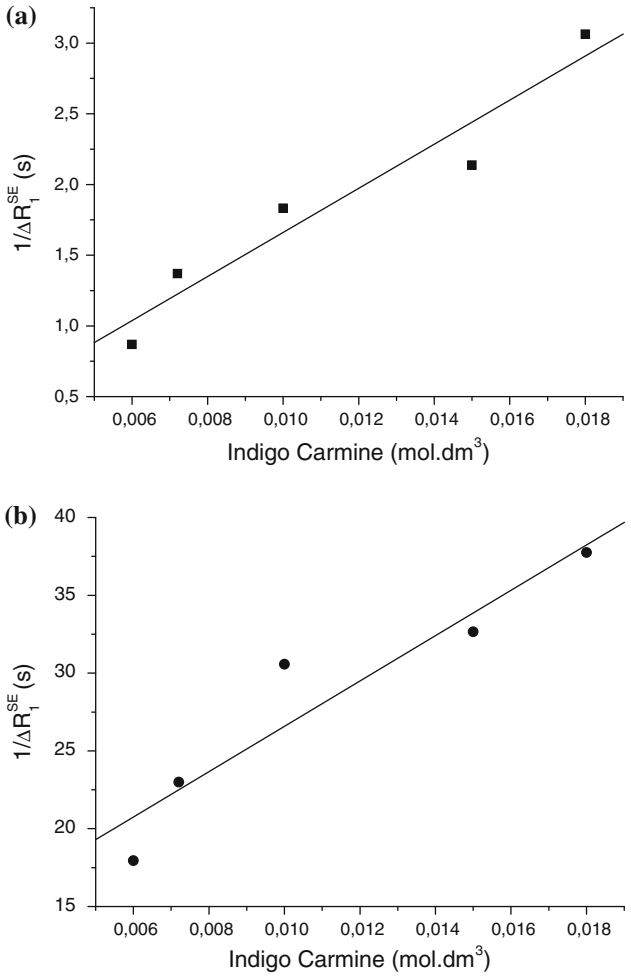

Fig. 6 Calculated values of $1/\Delta R_1^{SE}$ versus variable concentrations of indigo carmine and: **a** BSA, **b** DX. Both the values of K and R_{1b}^{SE} were calculated from the slope and the intercept of the straight line

with BSA compared to DX, confirming its higher affinity toward the plasma protein with respect to DX.

Conclusions

The efficiency of dyeing processes is strongly affected by the ability of the colorant to form stable adducts with textile fibers. Thus, the investigation of the interaction processes between dyes and macromolecules able to simulate the structure of textile may play an important role for understanding the dyeing properties of different materials. Nuclear magnetic resonance spectroscopy represents an useful tool to study the interaction processes occurring between small molecules and macromolecules, such as proteins and polysaccharides. Nuclear spin relaxation analysis constitutes a valid approach to determine the affinity of a ligand toward different macromolecules, being proton relaxation rate the parameter most affected by changes in molecular dynamics. To the best of our knowledge, we use for the first time an approach based on proton spin–lattice relaxation rate analysis applied to dye-macromolecule systems, to investigate interaction processes involving dyes and macromolecules able to reproduce fiber environment.

Data obtained in this study demonstrate that indigo carmine, one of the most used dye, show very different affinity toward albumin (used to simulate wool fiber) and dextran (used to reproduce cotton environment), quantified by the calculation of the affinity indexes and equilibrium constants of dye-macromolecule systems. These results can be interpreted in terms of diverse persistence of indigo carmine in wool and cotton fibers, as well as different efficiency of the dyeing processes.

Acknowledgements Authors would like to thank the University of Siena for financial support.

Disclosures All authors disclose any actual or potential conflict of interest including any financial, personal or other relationships with other people or organizations within 3 years of beginning the work submitted that could inappropriately influence their work.

References

1. Ahmed NSE, El-Shishtawy RM (2010) J Mater Sci 45:1143. doi:10.1007/s10853-009-4111-6
2. Knecht E, Rawson C, Loewenthal R (eds) (1933) A manual of dyeing, vols 1 and 2, 9th edn. Griffin C, London
3. Hill DJ (1997) Rev Prog Coloration 27:18
4. Kumar CV, Buranaprapuk A (1997) Angew Chem Int Ed Engl 36:2085
5. Sudlow G, Birkett DJ, Wade DN (1975) Mol Pharm 11:824
6. Bar-Or D, Lau E E, Winkler JV (2000) J Emerg Med 19:311
7. Flarakos J, Morand KL, Vouros P (2005) Anal Chem 77:1345
8. Carter DC, He XM, Munson SH, Twigg PD, Gernert KM, Broom MB, Miller TY (1989) Science 244:1195
9. Hushcha TO, Luik AI, Naboka YN (2000) Talanta 53:29
10. McNab H, Hulme AN, Ferreira ESB, Quye A (2004) Chem Soc Rev 33:329
11. del Rio MS, Boccaleri E, Milanesio M, Croce G, van Beek W, Tsiantos C, Chyssikos GD, Gionis V, Kacandes GH, Suarez M, Garcia-Romero E (2009) J Mater Sci 44(20):5524. doi:10.1007/s10853-009-3772-5
12. Balfour-Paul J (1998) Indigo. British Museum Press, London
13. Marmarion DM (1979) Handbook of US colorants for food, drugs and cosmetics. Wiley-Interscience, New York, p 265
14. Stewart I, Wheaton TA (1971) J Chromatogr 55:325
15. Wang Y, Wen YY, Ding HM, Shan YK (2010) J Mater Sci 45(5):1385. doi:10.1007/s10853-009-4096-1
16. Lui HW, Zhu T, Zhang YN (1995) J Chromatogr A 718:448
17. Bauer C, Freeman R, Frenkiel T, Keeler J, Shaka AJ (1984) J Magn Reson 58:442
18. Bloch F (1957) Phys Rev 105:1206
19. Solomon I (1955) Phys Rev 99:559
20. Noggle JH, Shirmer RE (1971) The nuclear overhauser effect. Academic, New York

21. Rossi C, Bastianoni S, Bonechi C, Corbini G, Corti P, Donati A (1999) Chem Phys Lett 310:495
22. Neuhaus D, Williamson M (1989) The nuclear overhauser effect in structural and conformational analysis. VCH Publisher, New York
23. Freeman R, Hill HDW, Tomlinson BL, Hall LD (1974) J Chem Phys 61:4466
24. Martini S, Bonechi C, Casolaro M, Corbini G, Rossi C (2006) Biochem Pharmacol 71:858
25. Martini S, Consumi M, Bonechi C, Rossi C, Magnani A (2007) Biomacromolecules 8:2689
26. Bonechi C, Martini S, Brizzi V, Brizzi A, Massarelli P, Bruni G, Rossi C (2006) Eur J Med Chem 41:1117
27. Meksi N, Kechida M, Mhenni F (2007) Chem Eng J 131:187
28. Komboonchoo S, Bechtold T (2009) J Cleaner Prod 17:1487
29. Nishida K, Akimoto T, Uedaira H (1969) Colloid Polym Sci 233:896
30. Nath RK, Singh ThC, Dasgupta S, Mitra A, Panda AK (2010) Mater Sci Eng C 30:549